Global Journal of Researches in Engineering: B
Automotive Engineering
Volume 14 Issue 4 Version 1.0 Year 2014
Type: Double Blind Peer Reviewed International Research Journal
Publisher: Global Journals Inc. (USA)
Online ISSN: 2249-4596 & Print ISSN: 0975-5861

Development a Single Zone Heat Release Model

By J. Alrajhi, M. Alardhi, A. Abed & K. Alkhulaifi
Collage of Technological Studies Public authority of Applied Education and Training-Kuwait, Kuwait

Abstract- Single zone heat release models can effectively be used to model diesel engine combustion process with acceptable degree of accuracy. These models are mainly depend on double Wiebe function which requires as many as six parameters in order to predict the heat release rate (HRR) accurately. However, Wiebe function does not look into the physical air fuel mixing process during the ignition delay (ID) which makes their predictions far from understanding the relation between the HRR and the physical interaction between air and fuel prior to combustion. Whitehouse and Way model covers the physical process since it deals with the mass of fuel injected and the partial pressure of oxygen in which the reaction rate is computed by an Arrhenius type expression. In this work, a strong relationship between HRR and air mass entrained during the ID has been shown. A new single zone heat release model based on Whitehouse and Way model for diesel engine has been developed in order to predict the HRR using standard diesel fuel. The new model has shown to give good results compared to experimental data.

Keywords: heat release model, single zone model, whitehouse and way model, direct injection, diesel engine.

GJRE-B Classification : FOR Code: 090104p

DEVELOPMENTASINGLEZONEHEATRELEASEMODEL

Strictly as per the compliance and regulations of :

Development a Single Zone Heat Release Model

J. Alrajhi [α], M. Alardhi [σ], A. Abed [ρ] & K. Alkhulaifi [ω]

Abstract- Single zone heat release models can effectively be used to model diesel engine combustion process with acceptable degree of accuracy. These models are mainly depend on double Wiebe function which requires as many as six parameters in order to predict the heat release rate (HRR) accurately. However, Wiebe function does not look into the physical air fuel mixing process during the ignition delay (ID) which makes their predictions far from understanding the relation between the HRR and the physical interaction between air and fuel prior to combustion. Whitehouse and Way model covers the physical process since it deals with the mass of fuel injected and the partial pressure of oxygen in which the reaction rate is computed by an Arrhenius type expression. In this work, a strong relationship between HRR and air mass entrained during the ID has been shown. A new single zone heat release model based on Whitehouse and Way model for diesel engine has been developed in order to predict the HRR using standard diesel fuel. The new model has shown to give good results compared to experimental data.

Keywords: heat release model, single zone model, whitehouse and way model, direct injection, diesel engine.

I. Introduction

Understanding the detailed physics and chemistry involved in the combustion processes of diesel engines are essential in predicting performance. Combustion process in diesel engines usually described [1] to consist of three main phases; premixed combustion, rate controlled diffusion combustion and late diffusion combustion. Experimental work is essential to understand the combustion process in diesel engines, and therefore provide relatively precise results for a specific test needed to ensure effective emission reduction. However, they are often uneconomical and time consuming. To overcome this, heat release models can effectively isolate one variable at a time and point out trends and causes.

Heat release models used for diesel engine combustion are classified into two groups, thermodynamic and multidimensional models. The thermodynamic models can be classified into three subgroups; single zone, two zones and multi zone models [2]. In single zone models, the entire volume of the combustion chamber is assumed to be a homogeneous mixture of air and combustion products and uniform in temperature. The first law of thermodynamics is used to calculate the mixture energy accounting for the enthalpy flux due to fuel injection. The fuel injected into the cylinder is assumed to mix instantaneously with the cylinder charge, which is assumed to behave as an ideal gas. At combustion, it then assumes that the fuel is burned immediately on injection into the combustion chamber [1, 3, 4, 5]. Often the measured pressure rise in an engine is used to tune the model or is used to provide a rate of heat release.

Although the assumption of homogeneous dispersion of the injected fuel is unrealistic, single zone models are valuable tools for quick analysis of the engine cycle and preliminary design computations.

One of the early single zone model was developed by Austen and Lyn [6]. This model emphasized the importance of the rate of fuel injection and indicated how the various phases of the combustion process may be dealt with mathematically. The model considered both the premixed and diffusion combustion phases while the combustion rate was obtained from the analysis of experimental cylinder pressure diagrams.

Another example of the early development of a single zone model for predicting the HRR in diesel engines are single and double Wiebe functions [7]. Since then many authors have used the single and double Wiebe functions in order to predict the average pressure and temperature in DI and IDI engines [8, 9 10, 11, 12].

For non-Wiebe type functions, Whitehouse and Way [4] developed a semi-empirical model for calculating rates of combustion in DI diesel engines which allow calculation of the fuel injection rate and the amount of oxygen available in the cylinder during the combustion process. In their model, the fuel preparation rate for ignition was assumed to be dependent upon the total surface area of the droplets forming the fuel spray. The effect of ignition delay was considered by introducing a chemical reaction rate using an Arrhenius type expression.

Carddock and Hussain [13] developed their single zone model based on experimental data obtained from their single cylinder highly charged diesel engine.

They also divided the combustion process into premixed and diffusion phases. Although their

Author α σ ρ: Department of Automotive & Marine Engineering. Collage of Technological Studies Public authority of Applied Education and Training-Kuwait, El-Shuwaikh, Kuwait.
e-mail: a.abed@paaet.edu.kw
Author ω: Department of Power and Air Conditioning, Collage of Technological Studies Public authority of Applied Education and Training-Kuwait, El-Shuwaikh, Kuwait.

correlation looks promising, it has many empirical coefficients which make it difficult to use.

In this work, a new single zone heat release model based on experimental data is developed by looking into the air mass entrained within the fuel spray during the ID. The proposed model assume that combustion process consist of two main phases; premixed and diffusion. The premixed combustion phase is further divided into two stages; accumulation and depletion, Figure 1.

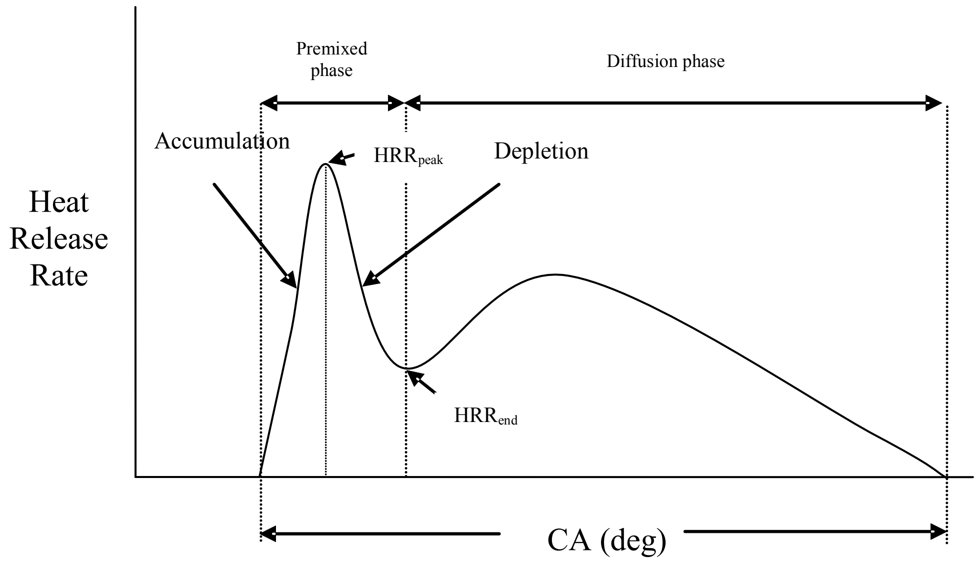

Figure 1 : The two combustion phases and the two premixed combustion stages considered for the new heat release model showing the peak and the end of premixed combustion phase

II. Heat Release Model Development

The development of the new model is based on the assumption that combustion processes will first occur in the air fuel mixture which will define the premixed phase. Before the end of the premixed combustion phase, the flame front will propagate towards the air mass surrounding the premixed phase initiating the diffusion combustion. From experimental data, the end of premixed combustion phase is shown in Figure 2 and is defined by the dotted line.

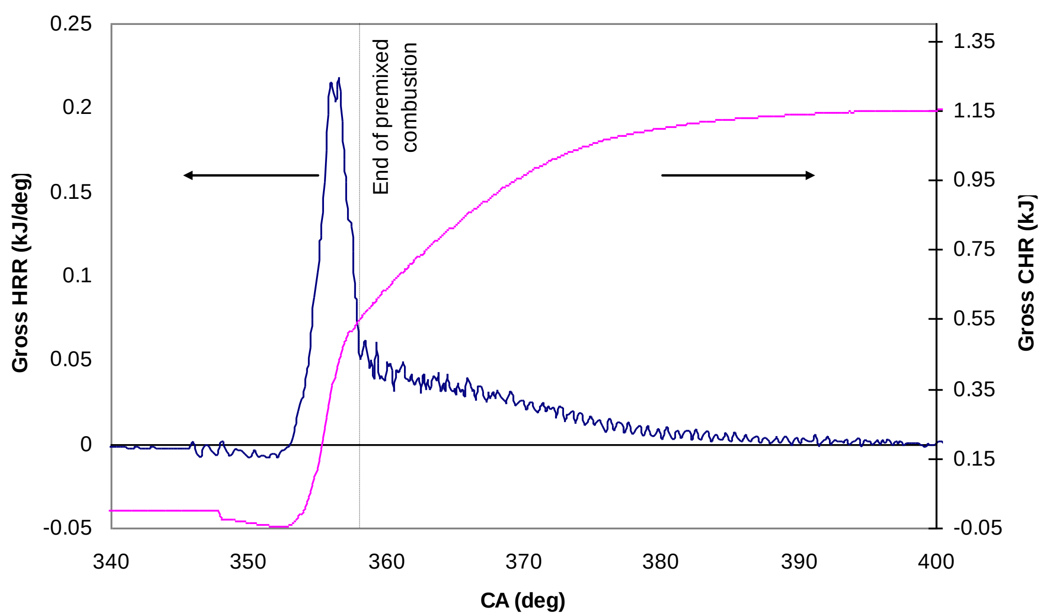

Figure 2 : Gross cumulative and heat release rate at 1200RPM and 150N.m using AD

From the cumulative heat release curve shown above, the energy released at the end of the premixed phase is 0.55 kJ and mass of fuel required to release this energy is 12.9 mg. However, the mass of fuel injected during ignition delay was 18.8 mg. This proves that not all the fuel injected during the ignition delay is burned during the premixed phase. Therefore the fuel mass injected during ignition delay is difficult to rely upon in order to predict the premixed combustion phase.

The prediction of premixed combustion phase for the new heat release model is based on the amount of air entrained during the ID within the air fuel mixture.

Figure 3 shows the plot of the gross HRR from the start of combustion until its peak value (HRRpeak), the calculated air mass entrained within the air fuel mixture from the start of injection (SOI) until the start of combustion (SOC) and the cumulative fuel injected from SOI to SOC.

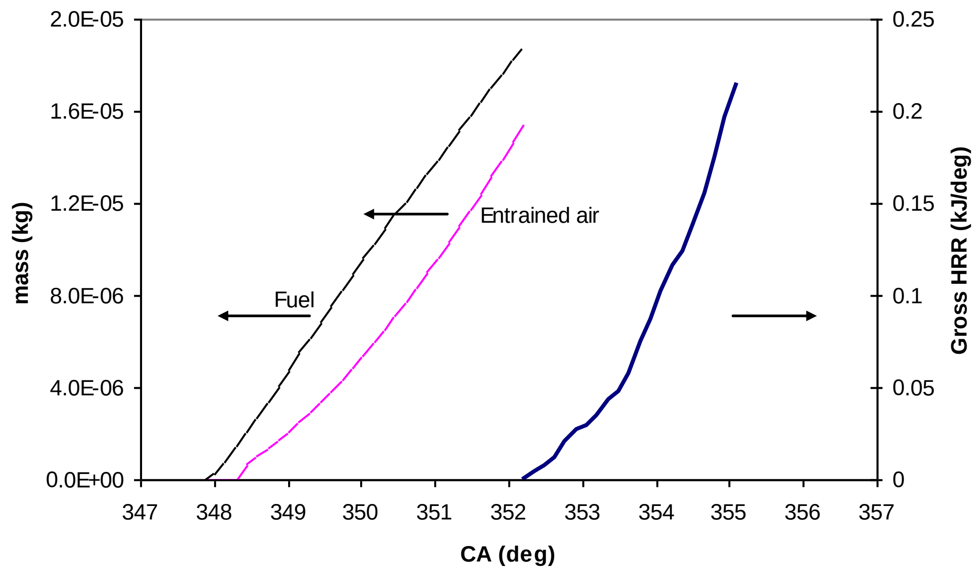

Figure 3 : Calculated air mass within the air fuel mixture formed during ID, cumulative fuel injected during ID and gross HRR from SOC until HRRpeak based on experimental parameters at 1200RPM and 150N.m using AD

The calculation of cumulative air mass entrained within the air fuel mixture is calculated knowing the fuel spray angle and penetration length as follows,

$$m_{air(M)} = \frac{\pi}{3}\tan\left(\frac{\phi_s}{2}\right)^2 \rho_{air}\,(X - X_{brs})^3 . \qquad (1)$$

Where:

ϕ_s is the spray angle

ρ_{air} air density

X Spray penetration length

X_{brs} is the breakup length with swirl effect

The time between SOI and the start of air entrainment is the break up time. Assuming injected fuel is in the vapor phase beyond the break up length, it is clear from Figure 3 that the air fuel mixture at any crank angle is fuel rich during the ignition delay.

The time lag between the air mass entrained and the HRR curves represent the ignition delay period minus the break up time. During this time the mixture is prepared for combustion.

Whitehouse and Way [14] explained this preparation time as the time for fuel to be heated and mix with a sufficient amount of oxygen for stoichiometric burning.

Although there is a similarity between the new heat release model which is about to be developed here and Whitehouse and Way preparation rate, their preparation rate was mainly rely on the amount of fuel prepared during ignition delay time. For the new model fuel is assumed to be always prepared during fuel injection process. Therefore, the entrained air will be used to describe the heat release rate. From the experimental parameters at 1200RPM and 150N.m using AD and by trial and error, fitting an exponent of 1.5 to the air mass entrained and an exponent of 0.1 to the cumulative fuel injected and using the product of air and fuel masses resulted in a correlation with the gross HRR curve during accumulation phase. In other words, the air mass entrained within the air fuel mixture and cumulative fuel injected can be correlated with the gross HRR accumulation phase. This assumes that during the delay between the SOI and SOC, the fuel and air mixes and become ready for combustion, Figure 4.

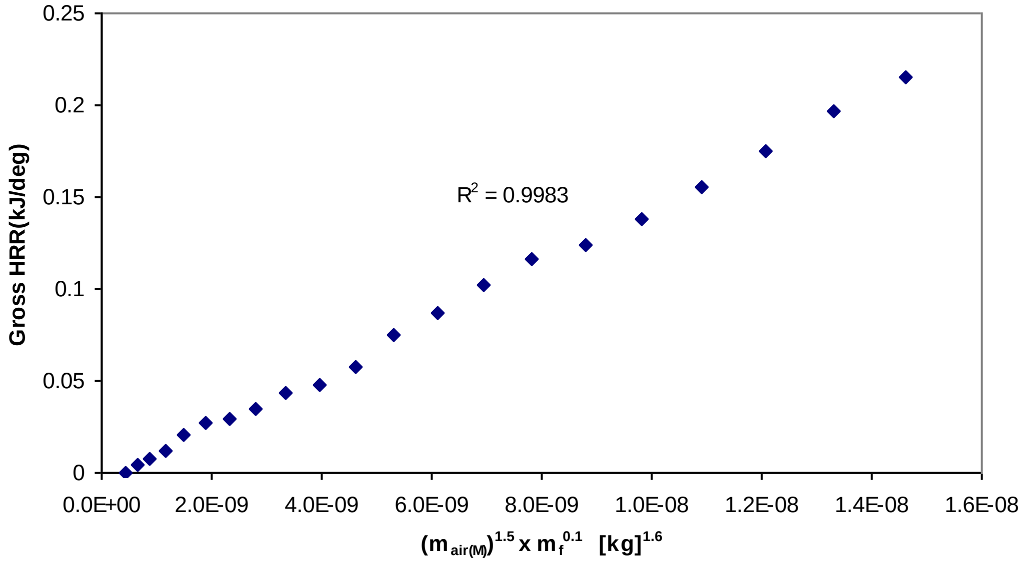

Figure 4 : Gross heat release rate during the accumulation phase versus air mass entrained during the ID to the power 1.5 and cumulative fuel injected during the ID at 1200RPM and 150N.m using AD

This was true for all test points during this study using standard diesel fuel. It is evident that the accumulation phase of the gross HRR is directly proportional to the mass of cumulative fuel injected and the mass of entrained air within the air fuel mixture during the ID. Then the gross HRR relationship becomes,

$$HRR_{prem} \alpha (m_{air(M)}^{1.5}\ m_f^{\ 0.1})\,. \tag{2}$$

Replacing the proportionality with a constant, then equation (2) becomes,

$$HRR_{prem} = K_{prem}\ m_{air(M)}^{1.5}\ m_f^{\ 0.1}\,. \quad \text{(kJ/deg)} \tag{3}$$

Where K_{prem} (kJ kg$^{-1.6}$ deg^{-1}) is an adjustable constant. By superimposing the air mass entrained curve over the *HRR$_{prem}$*, the gross HRR during the accumulation phase can be calculated using equation (3). The air mass can be calculated from equation (1) from the SOI until the SOC. Also the fuel mass is calculated from the SOI until the SOC. Once the maximum value of the air mass entrained during ID is reached (at SOC), the heat release rate peak is assumed to be reached. If combustion process is assumed to take place at stoichiometric conditions, the remaining air mass entrained within the air fuel mixture will then be subtracted from the burned air during each time step which will define the depletion phase as shown in the following equation,

$$m_{air(M)i} = m_{air(M)i-1} - m_{air(burned)} \tag{4}$$

Where $m_{air(M)i}$ is the unburned air mass entrained at present step and $m_{air(M)i-1}$ is at the previous step. The unburned fuel can be calculated similarly as the unburned air mass,

$$m_{f(i)} = m_{f(i-1)} - m_{f(burned)} + m_{finj(step)} \tag{5}$$

Where $m_{f(i)}$ is the mass of unburned fuel at present step and $m_{f(i-1)}$ is at the previous step. $m_{finj(step)}$ the mass of fuel injected during the time step. Equations (4) and (5) define the depletion stage during the premixed combustion phase (Figure 1). Once the fuel injection process ends, $m_{finj(step)}$ becomes zero. Figure 5 shows an illustration of the corresponding air and fuel masses accumulation and depletion trends during the premixed combustion phase.

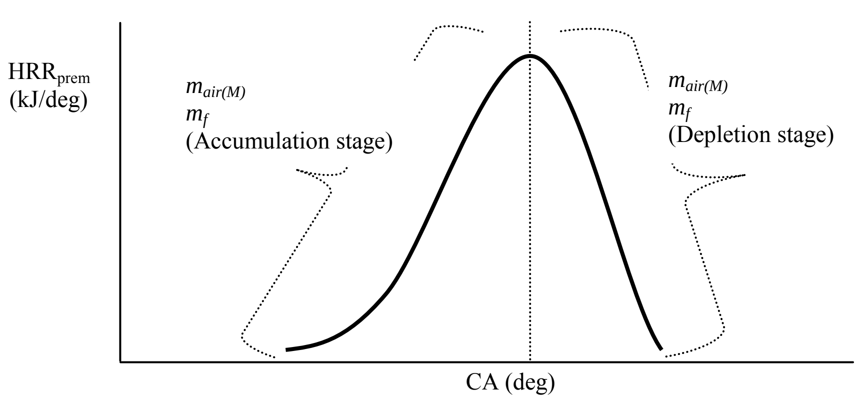

Figure 5 : The premixed combustion phase at the start of accumulation until the end depletion stages

The method used in developing the gross HRR during the premixed combustion phase is also followed for the diffusion combustion phase. The gross HRR from experimental data during the diffusion phase is plotted in Figure 6.

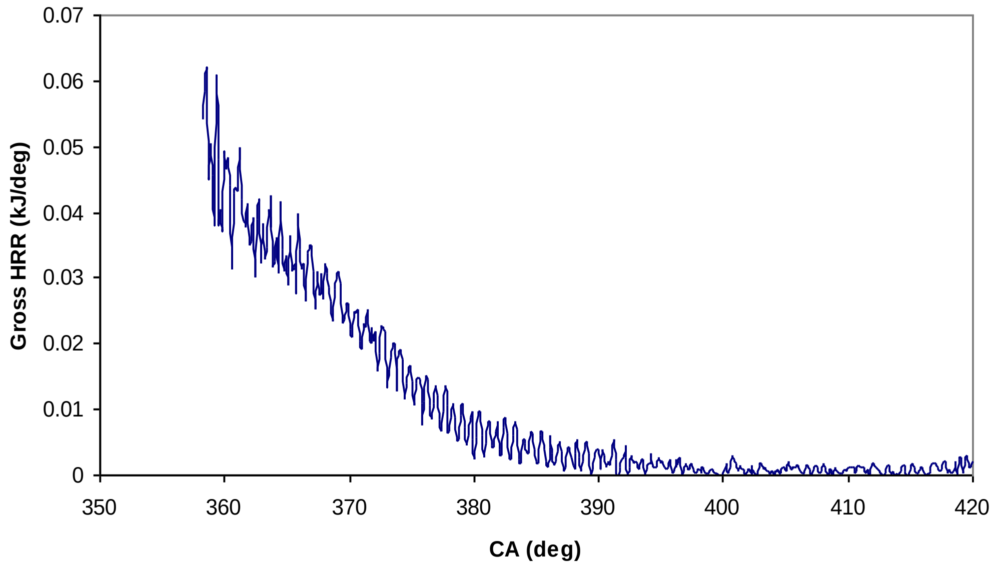

Figure 6 : The gross HRR during the diffusion phase at 1200RPM and 150N.m using AD

During the diffusion phase, the calculated unburned air mass within the cylinder from the experimental parameters is shown in Figure 7.

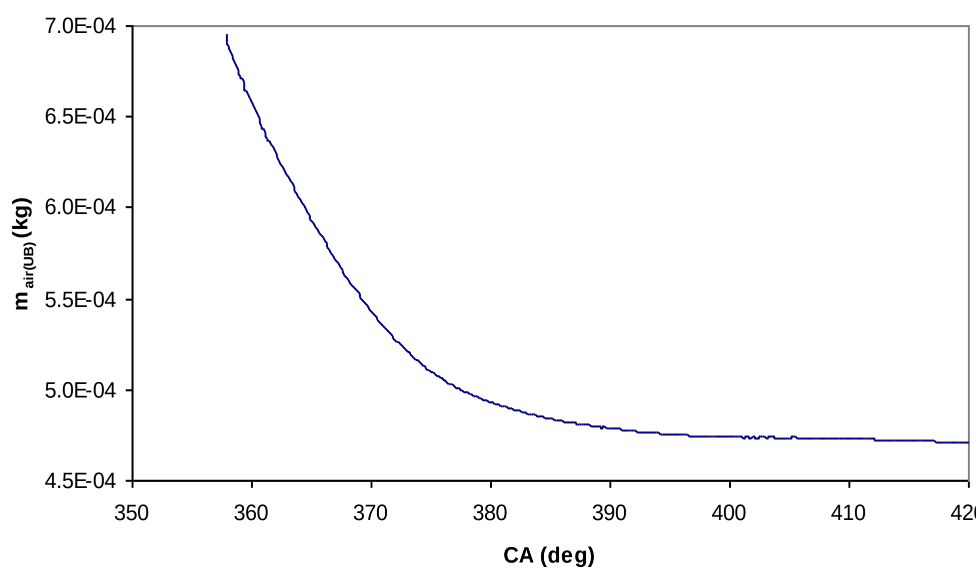

Figure 7 : The calculated unburned air mass from experimental parameters at 1200RPM and 150N.m using AD

Using an exponent of 0.5 for the unburned fuel, the unburned air and fuel masses can then be correlated with the HRR during the diffusion phase, Figure 8.

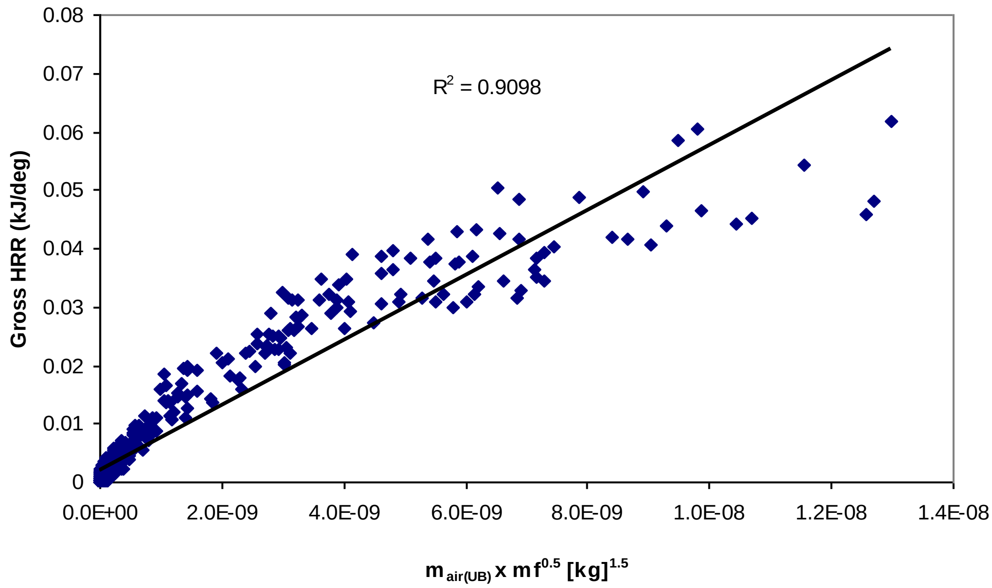

Figure 8 : The gross HRR during diffusion stage versus unburned air and fuel masses at 1200RPM and 150N.m using AD

Each data point in the above Figure represents the experimental gross HRR against the calculated air and fuel masses from the start of diffusion phase until it ends. The curve fit used for the diffusion phase for all test points is from the starting point of diffusion phase which is defined by the end of premixed combustion (Figure 2) until the end of combustion process. Since the fuel mass will define the end point of the diffusion combustion phase, the unburned fuel mass which did not react during the premixed combustion will be used in the diffusion combustion correlation. From the experimental data, the trend for the unburned fuel is similar to the mass of unburned air, Figure 9.

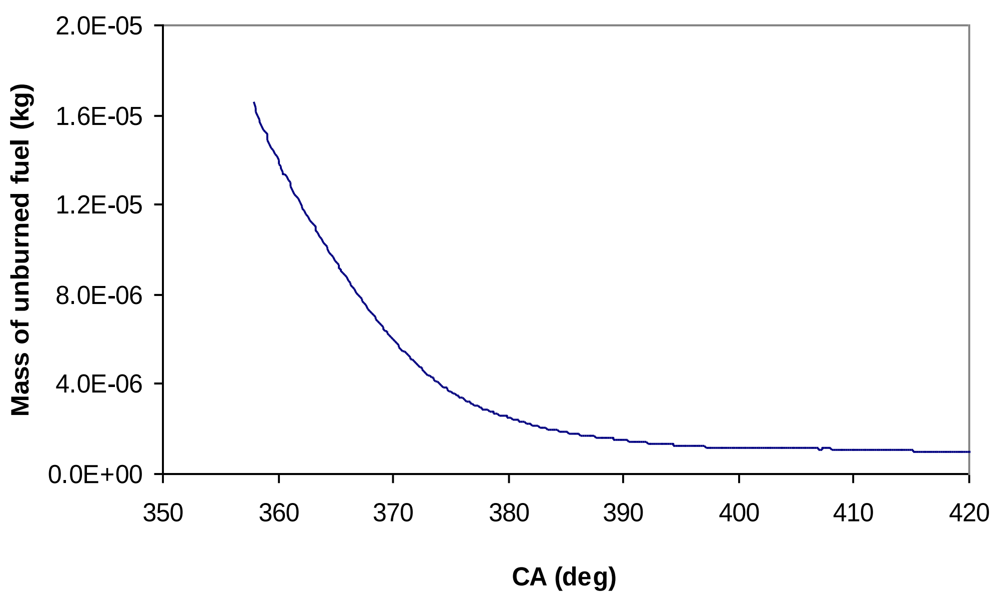

Figure 9 : The mass of unburned fuel during the diffusion phase at 1200RPM and 150N.m using AD

As it was the case with the premixed phase, the gross HRR during the diffusion combustion phase is directly proportional to the unburned air and fuel masses,

Global Journal of Researches in Engineering (B) Volume XIV Issue IV Version I Year 2014

$$HRR_{diff}\,\alpha(m_{air(UB)}\; m_f^{\;0.5})\,. \qquad (6)$$

Replacing the proportionality term with a constant, the final form of the heat release rate during diffusion phase is,

$$HRR_{diff} = K_{diff}\; m_{air(UB)}\; m_f^{\;0.5}\,.\;\; \text{(kJ/deg)} \qquad (7)$$

Where K_{diff} (kJ kg$^{-1.5}$ deg^{-1}) is an adjustable constant for the diffusion phase. In this case, equations (4) and (5) are to be used in equation (7) from the beginning until the end of the diffusion combustion. In equation (4), the remaining unburned air mass is used instead of the air mass within the air fuel mixture. At the beginning of the combustion cycle, the premixed HRR takes place first. Once the diffusion HRR is greater than the premixed HRR, the process is assumed to continue as a diffusion process until all fuel is completely burned,

$$HRR_{cycle} = \text{Max}\;(HRR_{prem},\, HRR_{diff}).\;\; \text{(kJ/deg)} \qquad (8)$$

Figure 10 shows the outcome of the HRR for the premixed phase (equation 3) and the diffusion phase (equation 8) shown above.

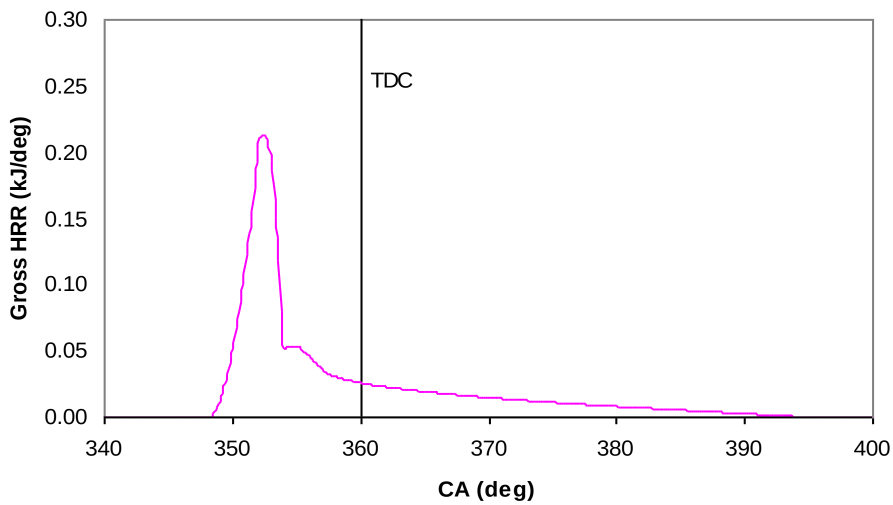

Figure 10 : Predicted gross HRR at 1200RPM and 150N.m using AD

From the SOC, the premixed phase dominates the combustion process. Once the HRR_{peak} isreached the diffusion phase starts to buildup while the premixed starts to deplete. Once thediffusion HRR becomes higher than the premixed, it dominates the combustion process until the end of the process. The constant K_{prem} is adjusted in order to match the peak HRR of the model to that of experimental data while K_{diff} is adjusted to have the best fit between the model and experimental diffusion curves. For this test point, K_{prem} and K_{diff} are 1.06E10^{7} (kJ kg$^{-1.6}$ deg^{-1}) and *1.40E10^{4}* (kJ kg$^{-1.5}$ deg^{-1}) respectively.

III. Experimental Setup

Experimental tests were conducted on four cylinders, 4.009L, Hino direct injection naturally aspirated medium speed diesel engine. The fuel injection system utilizes a BOSCH A-type in-line fuel pump and hole type injector nozzle. The engine was attached to an eddy-current dynamometer through an 80cm telescopic shaft. The dynamometer has a maximum power of 150 brake horsepower and maintains load on the engine by dissipating its mechanical power produced. The dynamometer controller is a Schenck electronic type which keeps the engine at a constant desired speed by varying the supply current to the dynamometer. The overall experimental setup is shown in Figure 11 while engine and injector specifications are listed in table 1.

Comparison between real and model heat release curves

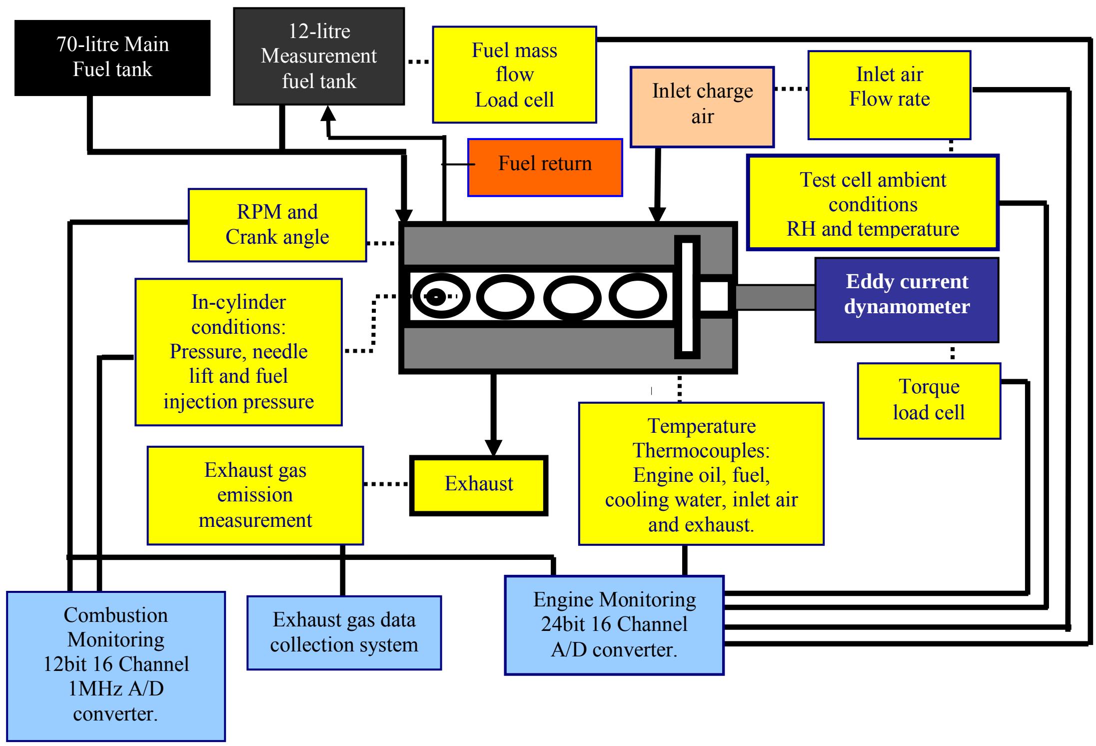

Figure 11 : Experimental Setup

Table 1 : Test engine specifications

Bore (B) x Stroke (l)	104 x 118(mm)
Compression Ratio (r)	17.9
Connecting rod length (L)	181.75 (mm)
Injector Nozzle (D_n)	5 holes x 0.29 mm dia x 160 deg cone angle
Needle opening pressure	215BAR
Valve timing	IVO (8^0 BTDC) – IVC (48^0 ABDC) EVO (60^0 BBDC) – EVC (8^0 ATDC)
Fuel pump plunger	9.5 mm dia x 8 mm max. stroke
Piston bowl shape	Toroidal

Three data acquisition systems were used to gather and record engine data. The engine performance data acquisition 24 bit, 1HZ National Instruments system was used to monitor and record engine load, air and fuel flow rates (turbine flow meter), relative humidity, and engine exhaust, fuel, inlet air, engine oil and coolant temperatures. The intake manifold was instrumented with an absolute pressure transducer with 0-1.6BAR range and 0-5v output and a K-type thermocouple. The fuel flow mass was gravimetrically measured using a 20kg “S” beam load cell (model LC-1205-K020) loaded in tension which can take up to 20kg of fuel mass. Knowing the air and fuel flow rates it is possible to determine the overall equivalence ratio for any test point. Humidity was measured using a capacitive humidity sensor (model EE06-A) with 0-100% range and 0-1V output. A thermocouple was placed in the exhaust manifold near the exhaust valve to measure the exhaust temperature and to compare later with the model temperature at the end of the expansion stroke. Another thermocouple was also used to measure engine coolant temperature and was used as a reference to determine when the engine reaches a steady state condition. All the thermocouples used were of K-type.

The second data acquisition system was used to monitor and record cylinder pressure, needle lift and fuel injection pressure readings at each crank angle position. An AVL piezoelectric high-pressure transducer (model GU12P) was mounted in the unused glow plug of cylinder number one for recording cylinder pressure. The fuel pressure was measured using an AVL fuel line high-pressure transducer (model SL31D-2000) mounted 50mm away from the injector in order to minimize fuel pulsations in the fuel pressure data. A third AVL sensor was used for monitoring the needle lift. The output of the transducers and the needle lift sensor were all fed to charge amplifiers, which convert the charge output to a voltage.

This voltage was fed to a data acquisition board capable of simultaneous sampling multi channels at 233kbps rate. This data acquisition board communicates with a personal computer through the parallel port. The crank angle position was measured using an optical encoder mounted on the front pulley of the crankshaft. The encoder has two-channels; one channel provides a pulse at top dead center while the other gives a pulse every 0.1deg of crank angle. The second data acquisition system output signals were all fed into an AVL Indimeter 619, which was used for continuous engine monitoring. The Indimeter 619 output signal was acquired using a PC with AVL Indicom software, which records and visualizes the in-cylinder data at each pulse. This gives 7200 data points for each cycle.

The third acquisition system used was a CODA exhaust gas analyzer. It measures and records NO_x (ppm), CO (%), CO_2 (%), HC (ppm) and O_2 (%) by means of chemiluminescence and electro-chemical cells. The CODA analyzer was also capable of reading lambda (air fuel ratio) based on the CO_2 and O2 exhaust measurements. Exhaust emissions especially NO_x readings were used to determine when the engine reaches steady state condition since they are more sensitive to the stability of combustion temperature.

IV. Model Validation

For a baseline test, the authors operated the engine at six speeds with two loads for each engine speed using standard diesel fuel as shown in table 2.

Table 2 : Speeds and loads considered in this work

Engine speed (RPM)	Load (N.m)	
1200	150	200
1400	150	200
1600	150	200
1800	150	200
2000	150	200
2200	150	200

Each test point data represents an ensemble average of three sample points for the engine performance data per indicated value whereas the in-cylinder measurements represent an ensemble average of 10 cycles. The model was first verified against experimental work using standard diesel fuel. The heat release model adjustable constants and swirl ratio are set at their optimum values in order to have the best match between experimental and predicted cylinder pressure and heat release data. The reason of doing this is to correlate the premixed and diffusion adjustable constants to the engine operating conditions. The HRR from the new model has shown to be in a good agreement with the experimental data as it is expected since adjustable constants were adjusted to match the experimental data.

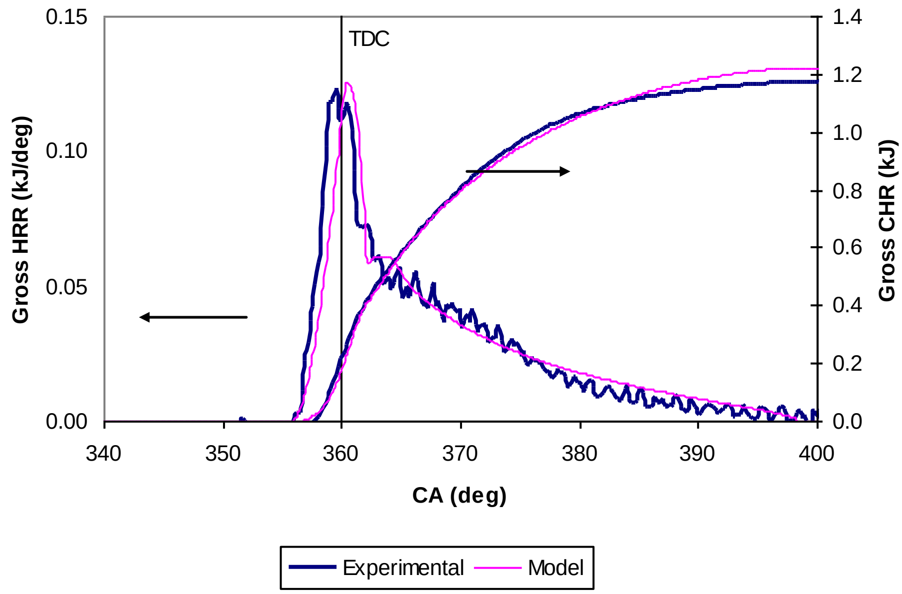

Figure 12 : Experimental and predicted cumulative and rate heat release using optimum premixed and diffusion constants at 1800RPM and 150N.m

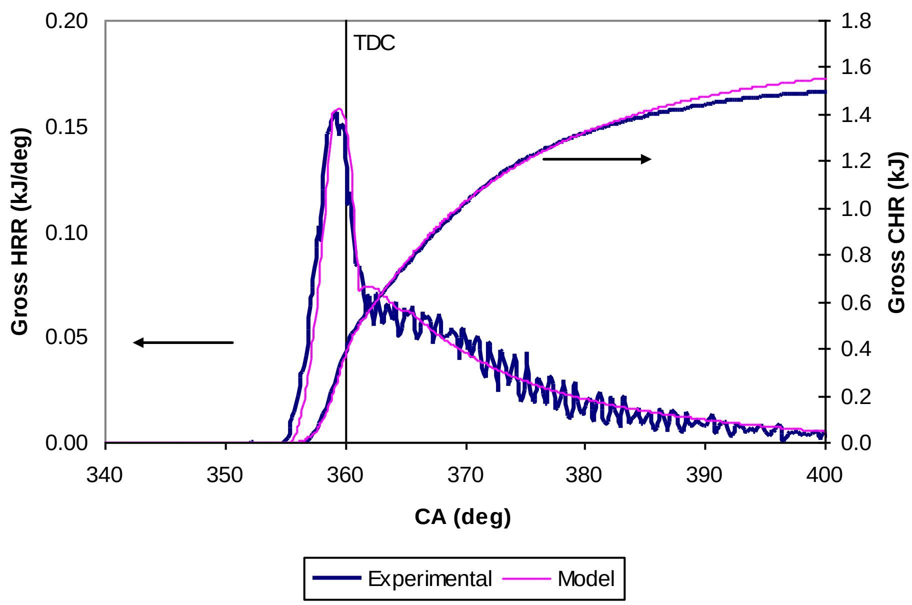

Figure 13 : Experimental and predicted cumulative and rate heat release using optimum premixed and diffusion constants at 1800RPM and 200N.m

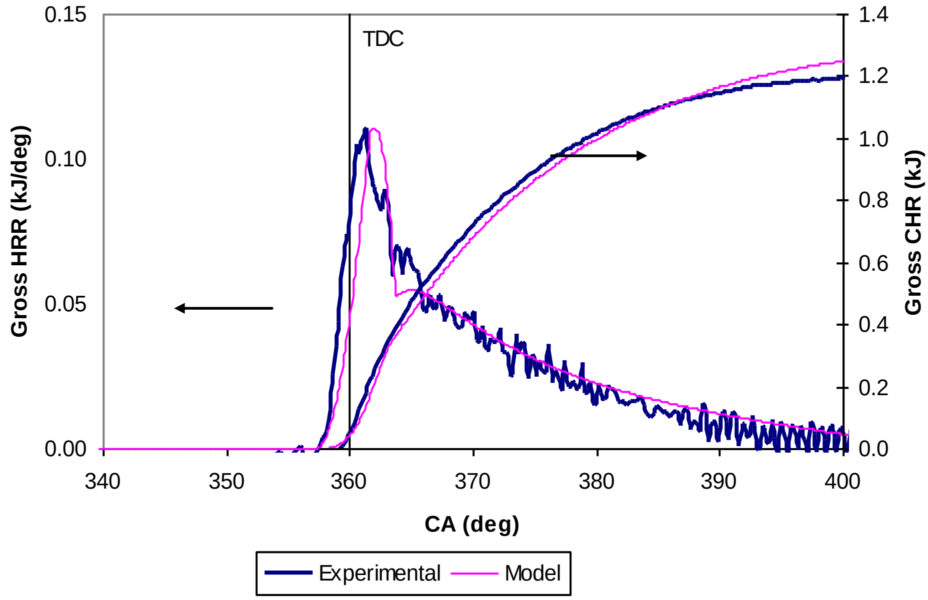

Figure 14 : Experimental and predicted cumulative and rate heat release using optimum premixed and diffusion constants at 2200RPM and 150N.m

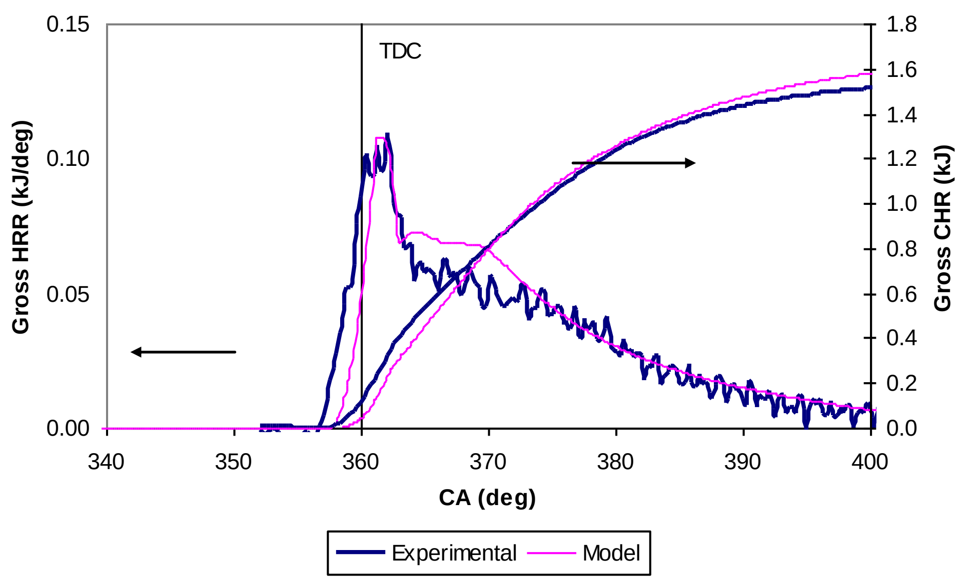

Figure 15 : Experimental and predicted cumulative and rate heat release using optimum premixed and diffusion constants at 2200RPM and 200N.m

The offset between the predicted and experimental HRR data is due to the difference between the experimental and correlated ID. The duration of the predicted premixed combustion phase agrees well with that of the experimental data especially at lower engine load. At 200N.m load, the predicted duration of the premixed combustion phase is shorter than that of the experimental data. The model adjustable constants and swirl ratio at their optimum values used for the above cases are shown in table 3.

Table 4 : Optimum heat release model constants for the above cases

RPM	Load	Kprem.	Kdiff.	Swirl ratio
1800	150	7.01E+06	1.70E+04	9.0
	200	5.74E+06	2.12E+04	5.0
2200	150	6.16E+06	1.62E+04	6.0
	200	5.53E+06	2.12E+04	5.0

V. Heat Release Model Calibration

In the previous section, the heat release adjustable constants in the model were set at their optimum values for each case to obtain the best fit between the experimental and predicted cylinder pressure and heat release rate curves. At this point it is worthwhile to investigate the correlation between these constants in the model and engine operating conditions. From the modelling results, it was noted that the premixed adjustable constant Kprem at their optimum values is dependent on the average difference between the fuel injection pressure and cylinder pressure. This finding motivated an attempt to correlate one against the other, Figure 16.

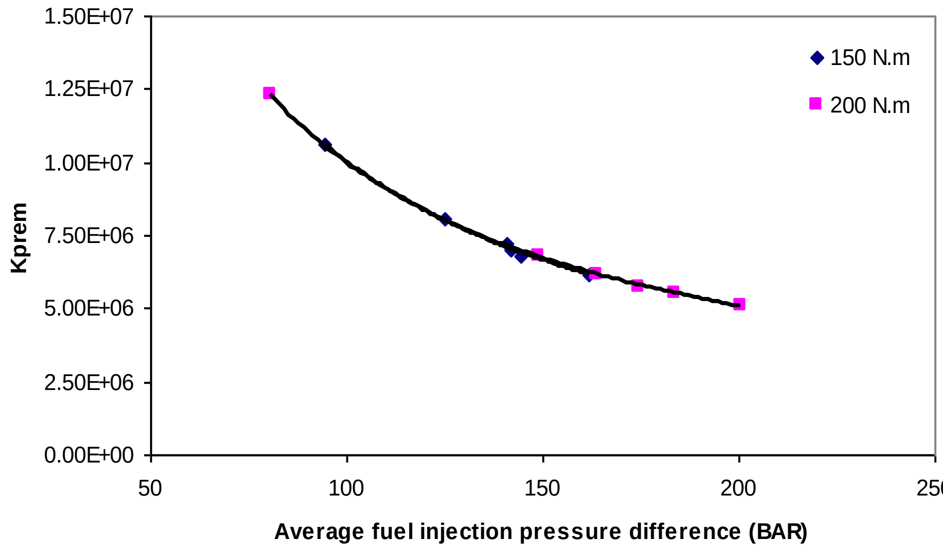

Figure 16 : The dependence of optimum Kprem on average fuel injection pressure difference for the two loads and all engine speeds

The two fitted lines have similar trends and slopes. For the 200N.m, K_{prem} values have bigger variation throughout the range of engine speeds and marginally higher than that of 150N.m. The data points at 150N.m are more clustered than at 200N.m. The average fuel injection pressure difference was found while holding the nozzle discharge coefficient at *0.70.* Taking the average of the above two curves gives an estimation of K_{prem}, Figure 17.

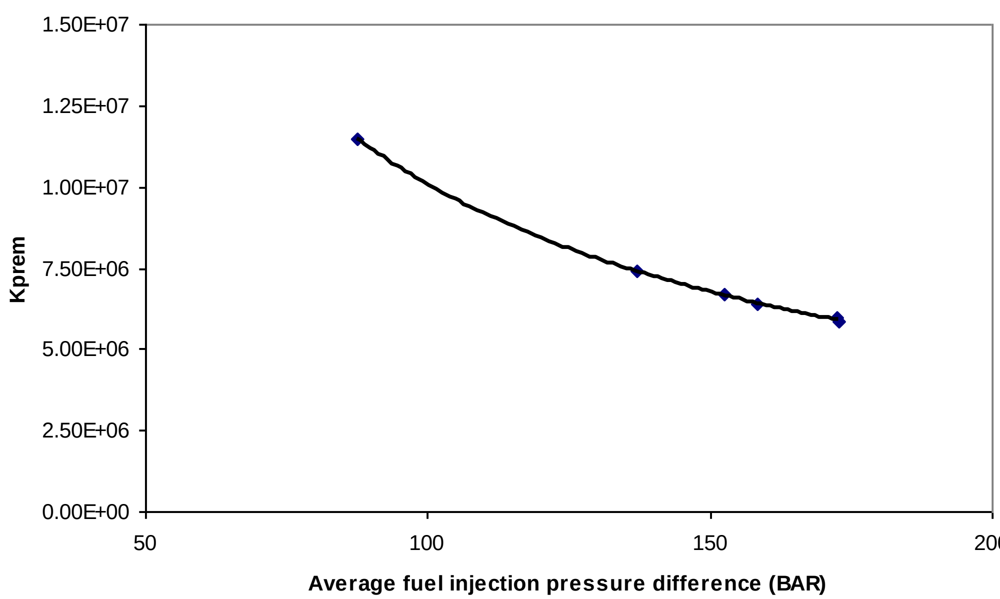

Figure 17 : Average values of K_{prem} and fuel injection pressure difference at all engine speeds and both loads

Using a power line fit to the data of Figure 17, the premixed adjustable constant can now be calculated using the following general correlation,

$$K_{prem} = 1.0 \times 10^{9}\ \Delta P^{-1.0} \qquad (9)$$

Where ΔP P is the calculated average fuel injection pressure difference (BAR). The above correlation can now be used to recalculate K_{prem} as shown in table 5.

Table 5 : The calculated premixed adjustable constant for the fitting cases

RPM	Load	Kprem	
		Optimum values	Calculated values
1800	150	7.01E+06	7.05E+06
	200	5.74E+06	5.73E+06
2200	150	6.16E+06	6.18E+06
	200	5.53E+06	5.45E+06

For the above cases the variation range between the optimum and calculated values of K_{prem} is less than 3%. Other test points also showed good agreement between the optimum and calculated premixed adjustable constant (within 3% variation).

Similarly plotting the diffusion adjustable constant Kdiff at their optimum values at all engine speeds and both loads using AD is shown in Figure 18.

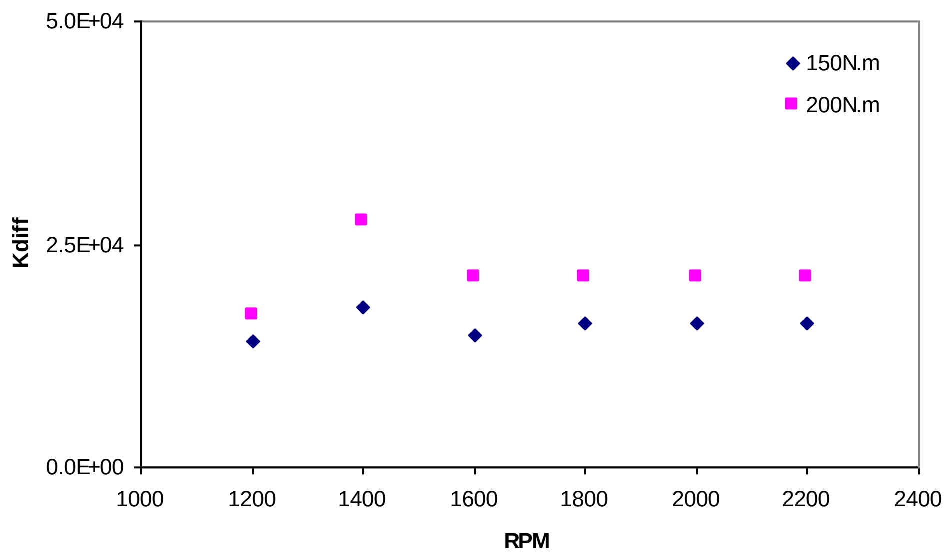

Figure 18 : The optimum diffusion adjustable constant values at all engine speeds and both loads

The trends of both loads are almost constant throughout the whole engine speed range while higher load has higher K_{diff} values. For the diffusion adjustable constant, no specific trend could be found with the fuel injection pressure difference as it was the case with K_{prem}. Therefore, an average value of K_{diff} is used in this case. At 150N. m the average K_{diff} is 1.59 E+4 while at 200N.m it is 2.16E+4. The overall average for both loads is 1.87E+4. The maximum variation between the overall average and the optimum diffusion adjustable constant is 18% which occurs at 150N.m. Figures 19 and 20 shows the effect of the variation with the averaging technique on HRR and cylinder pressure curves during the diffusion phase.

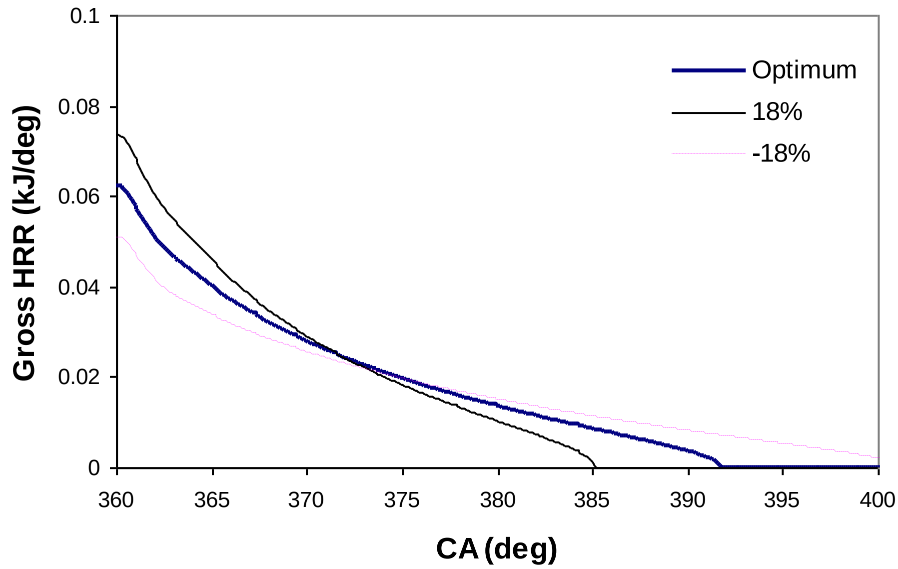

Figure 19 : The gross HRR during the diffusion phase with +/- 18% variation between the optimum adjustable diffusion constant and the overall average constant at 1800RPM and 150N.m

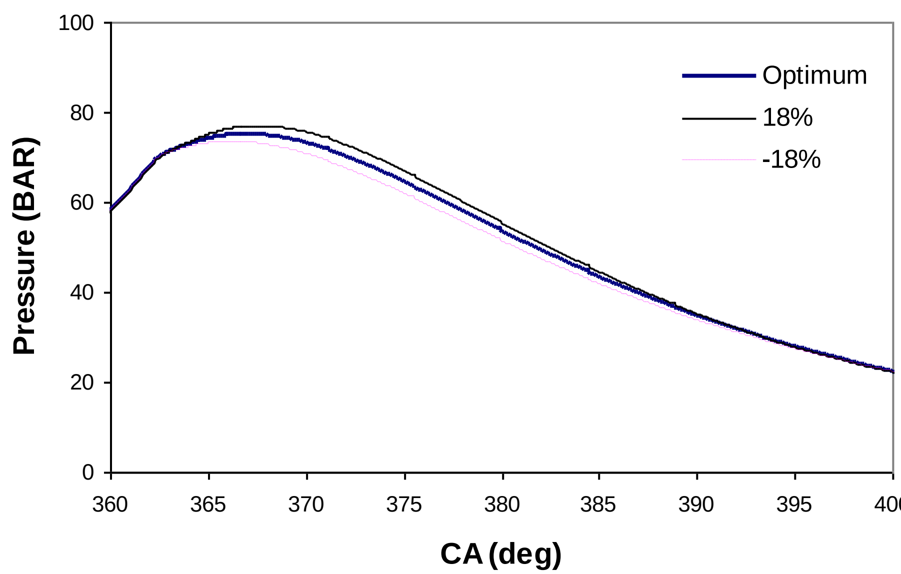

Figure 20 : Cylinder pressure curves with +/- 18% variation between the optimum adjustable diffusion constant and the overall average constant at 1800RPM and 150N.m

The 18% variation in the diffusion phase resulted in 2.6% variation in the cylinder pressure values. In this case the overall average of the diffusion adjustable constant can be used with the expectation of small variation in cylinder pressure readings. Other test points showed better agreement between predicted and experimental pressure and temperatures curves.

VI. Conclusion

A simple method for a single heat release model based on experimental heat release and fuel injection pressure data has been developed. The model uses an Arrhenius based expression to evaluate the rate of premixed and diffusion phases. The premixed phase has been breakup into accumulation and depletion phases using the fuel and air masses mixed and prepared during the ID. The diffusion phase has been developed using the unburned fuel and air. Fuel injection pressure was then used to predict the constants in the newly developed heat release model. The model has successfully predicted the heat release rate hence cylinder pressure and temperature with acceptable margin of error. The model developed offers a stable and accurate platform to calculate the HRR for diesel engine under various operating conditions using standard diesel fuel.

References Références Referencias

1. Heywood, J., *Internal Combustion Engine Fundamentals.* 1988.
2. Abdalla, G., Soliman, O. and Abd-Rabo, M., *Combustion Quasi-Two Zone Predictive Model for Duel Fuel Engines.* Energy Conversion and Management, 2001. 42(12): p. 1477-1498.
3. Austen, H. and Lyn, W. T., *The Application of Heat Release Analysis to Engine Combustion Study.* Proc. of CIMAC, 1962: p. 1067.
4. Carddock, J. and Hussain, M., *A Rate of Heat Release Correlation for Highly Charged Diesel Engines.* SAE 6860083, 1986.
5. Dychenko, N.X., Magedovich, L.E. and Pougachov, B.P., *Determination of Parameters of Heat Release Characteristic During Combustion in Diesel Engine.* Troudi, 1970(LPI 316).
6. Foster, D.E., *An Overview of Zero -Dimensional Thermodynamic Models for Ic Engine Data Analysis*. SAE 852070, 1985.
7. Ghojel, J., *A Study of Combustion Chamber Arrangements and Heat Release in Di Diesel Engines.* SAE 821034, 1982.
8. Miyamoto, N., Chikahisa, T., Murayama, T. and Sawyer, R., *Description and Analysis of Diesel Engine Rate of Combustion and Performance Using Wiebe's Function*. SAE 850107, 1985.
9. Ramos, J.I., *Internal Combustion Engine Modeling.* 1989, New York: Hemisphere Publishing.
10. Shipinski, J., Uyehara, O. and Myers, P., *Experimental Correlation between Rate of Injection and Rate of Heat Release in a Diesel Engine*. ASME, 1968(68-DGP-11).
11. Whitehouse, N.D. and Way, R., *Rate of Heat Release in Diesel Engines and Its Correlation with Fuel Injection Data*. Proc. Inst Mech Engrs, 1970. 184(3J): p. 17-27.
12. Whitehouse, N.D. and Way, R.J.B., *Simple Method for the Calculation of Heat Release Rates in Diesel Engines Based on the Fuel Injection Rate*. SAE 710134, 1971.
13. Wiebe, I.I., *New Insight into the Engine Cycle*. 1962, Moscow: Mashgiz.
14. Woschni, G. and Anisits, F., *Experimental Investigation and Mathematical Presentation of Rate of Heat Release in Diesel Engines Dependent Upon Engine Operating Conditions.* SAE 740086, 1974.

Global Journal of Researches in Engineering (B) Volume XIV Issue IV Version I Year 2014

This page is intentionally left blank